

Ultrafast Charge Recombination of Photogenerated Ion Pairs to an Electronic Excited State

Ana Morandeira, Laurine Engeli, and Eric Vauthey*

Department of Physical Chemistry, University of Geneva, 30 quai Ernest Ansermet, CH-1211 Geneva, Switzerland

Received: December 3, 2001; In Final Form: February 13, 2002

The dynamics of charge recombination (CR) of ion pairs formed upon electron-transfer quenching of Zn tetraphenylporphine (ZnTPP) in the S_2 state has been investigated by fluorescence upconversion. These ion pairs have two possible CR pathways: (A) a highly exergonic CR to the neutral ground state and (B) a moderately exergonic CR leading to the formation of ZnTPP in the S_1 state. Upon addition of quencher, the S_2 fluorescence decreases considerably, while the S_1 fluorescence is unaffected, indicating unambiguously that CR occurs via path B. A large fraction of the S_2 fluorescence quenching occurs in less than 100 fs. CR to the S_1 state of ZnTPP takes place with time constants around 400 fs.

Introduction

One of the few remaining open questions in bimolecular photoinduced electron transfer (ET) reactions concerns the absence of the inverted region, predicted by Marcus theory,¹ in the high exergonicity regime.² Several hypotheses have been proposed to account for this discrepancy.^{3–5} It has been shown that an increase of the quenching distance with increasing exergonicity of the ET process, ΔG_{ET} , can shift the appearance of the inverted regime to more negative free energies.⁴ However, the distance seems not to be able to realistically explicate the absence of inversion for ΔG_{ET} below -2 eV.⁶ A complementary explanation is that, in this case, the reaction product is formed in an electronic excited state. The product of an ET between closed-shell neutral reactants, a *charge separation* (CS), is a pair of open-shell radical ions. The nonexistence of any report, to our knowledge, of the formation of excited radical ions in a highly exergonic CS does not, however, invalidate this hypothesis. Excited radical ions are indeed very difficult to detect in the condensed phase because, first, most of them do not fluoresce,⁷ and second, most of them are very short-lived.^{8,9} This is due to the weak oscillator strength and to the low energy of the first electronic transition of many aromatic radical ions.¹⁰

This problem does not occur for charge recombination (CR) of a geminate ion pair (GIP), where the product is a pair of closed-shell molecules. In most cases, however, the only electronic excited state located below the ion pair is a triplet state. If the GIP is generated by ET quenching of the singlet excited precursor, it is also in a singlet state and CR to the triplet excited state is spin-forbidden. In this case, CR predominantly occurs toward the neutral electronic ground state.^{11–13} If the excited reaction partner of the ET quenching is in the triplet state, the ensuing GIP is also in the triplet state and CR to the neutral ground state is spin-forbidden.^{14–16} We have recently shown that a very efficient spin-allowed CR of the triplet GIP occurs if the triplet state of the quencher is located below the GIP state.¹⁷ The net result of this ET quenching process is similar to a triplet energy transfer, but the electron exchange is not simultaneous but stepwise.¹⁷ On the other hand, if the triplet state of the quencher is located above the GIP state, the only

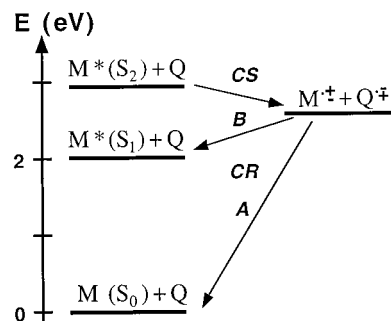


Figure 1. Energy diagram of the states involved in the photoinduced ET of ZnTPP (M) with a quencher (Q).

CR pathway is spin-forbidden and is thus very slow.¹⁸ In polar solvents, this situation results in the formation of free ions with a high quantum yield.^{14,15,19}

A situation where the GIP state is located above the singlet excited state of one of the reaction partners is more difficult to realize experimentally. This is nevertheless possible by electrochemical generation of the ions.²⁰ In this case, however, the ions are not spin-correlated and therefore both singlet and triplet GIPs are generated. A better approach, which avoids this complication, is to perform photoinduced ET between a reactant in an upper singlet excited state and a weak quencher. We have very recently reported on an investigation of the ET quenching of azulene (AZ), benzazulene (BA), and xanthione (XA) by weak donors in acetonitrile.²¹ As shown in Figure 1, there are two spin-allowed CR pathways in the resulting GIPs: (A) a highly exergonic CR to the neutral electronic ground state and (B) a moderately exergonic CR to the neutral precursors but with one reactant in the S_1 state. Our results showed strong indications of the predominance of path B. However, due to the very short lifetime and the lack of fluorescence of AZ, BA, and XA in the S_1 state, the occurrence of CR to an electronic excited state could not be totally unambiguously proved.²¹

We report here on our investigation of the dynamics of CS of Zn tetraphenylporphine (ZnTPP) in the S_2 state with weak quenchers and on the ensuing CR, using ultrafast fluorescence upconversion. Contrary to AZ, BA, and XA, ZnTPP has a long-lived and fluorescent S_1 state and therefore the occurrence of CR of the GIP to ZnTPP*(S_1) + Q can be univocally proved.

* Corresponding author: e-mail eric.vauthey@chiphys.unige.ch.

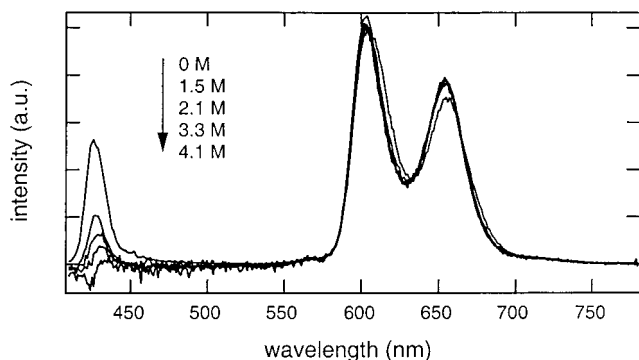


Figure 2. Steady-state fluorescence spectra of ZnTPP with various amounts of TMB in ACN (excitation at 400 nm), after subtraction of the Raman bands measured with the ACN/TMB mixtures alone.

Experimental Section

Measurements. The fluorescence upconversion setup was based on a FOG100 system (CDP Lasers & Scanning Systems). The light source was a Kerr lens mode-locked Ti:sapphire laser (Tsunami, Spectra-Physics) pumped by a Nd:YVO₄ laser (Millenia, Spectra-Physics). The output pulses between 800 and 840 nm had a duration of 80–100 fs and a repetition rate of 82 MHz. About 300 mW of this output was frequency-doubled in a 0.5 mm type I BBO crystal. The frequency-doubled pulses were focused on the sample located in a rotating cell, resulting in a pump intensity of about 10^{14} photons·cm⁻²·pulse⁻¹. The fluorescence was collected with an achromatic doublet. The unconverted pulses were sent along an optical delay line before being focused together with the fluorescence on a 0.5 mm type I BBO crystal. The polarization of the pump pulses was at the magic angle relative to that of the gate pulses at 800 nm. The upconverted signal was sent into a spectrograph and its intensity was measured with a photomultiplier tube operating in the photon counting mode. The full width at half-maximum (fwhm) of the response function of the setup was 210 fs.

UV–Vis absorption spectra were recorded on a Cary 50 spectrophotometer, and emission spectra were measured with a Cary Eclipse fluorometer.

Samples. Zn tetraphenylporphine (ZnTPP) was prepared from the free-base tetraphenylporphine and was subsequently purified by column chromatography. 1,2,4-Trimethoxybenzene (TMB) was distilled, while acetophenone (ACP), acetonitrile (ACN), and toluene (TOL) were of the highest commercially available grade and were used without further purification.

The concentration of ZnTPP was adjusted to obtain an absorbance at 400 nm of 0.1 on 0.4 mm, the sample thickness. This corresponds to concentrations of about 5×10^{-5} M. No significant degradation of the sample was observed after the upconversion measurements.

Results

Steady-State Fluorescence. Figure 2 shows the steady-state fluorescence spectrum of ZnTPP in ACN upon excitation at 400 nm. The bands at 605 and 650 nm are due to S₁ fluorescence, while the 430 nm band is S₂ fluorescence. ZnTPP is one of the few exceptions to exhibit fluorescence from an upper excited state.²² This is caused first by the very large S₀ → S₂ transition dipole moment and second by an inefficient S₂–S₁ internal conversion, due to the fact that the potential energy surfaces of both states are nearly parallel.²³ In TOL, the emission spectrum of ZnTPP is essentially the same as in ACN, except that the S₂ fluorescence quantum yield is smaller.

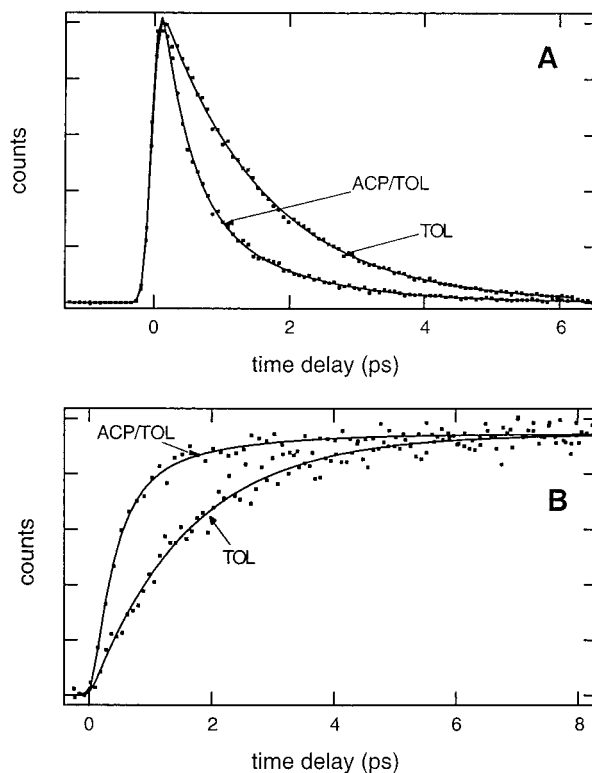


Figure 3. Intensity-normalized time profiles of the fluorescence intensity measured with ZnTPP at 430 nm (A) and 605 nm (B) in TOL and in a 1:1 mixture of ACP/TOL.

Figure 2 shows that, upon addition of large amounts of TMB, the S₂ fluorescence intensity is substantially reduced. On the other hand, the intensity of the S₁ emission is essentially unaffected. At 4 M TMB, the S₂ fluorescence is almost completely quenched, while the S₁ spectrum is just slightly blue-shifted. Qualitatively similar behavior was observed in TOL.

These measurements have also been performed in ACN and TOL with ACP as quencher. In both solvents, the addition of ACP results in the decay of the S₂ emission band, while the S₁ band remains essentially unchanged.

The absorption spectrum of ZnTPP is not affected by the addition of large amounts of quencher, and no new band that could indicate the formation of a complex was observed.

Time-Resolved Fluorescence. Figure 3A shows the S₂ fluorescence dynamics of ZnTPP in TOL upon excitation at 400 nm. The solid line is the best fit of the convolution of the instrument response function with a single-exponential decay with a lifetime of 1.53 ± 0.05 ps. This value is in close agreement with previous measurements in TOL.²⁴

In ACN, the S₂ fluorescence lifetime of ZnTPP is substantially longer (see Figure 4A) and amounts to 2.41 ± 0.05 ps, close to the value already reported in the literature.²⁴

Figure 3B shows the early dynamics of the S₁ fluorescence in TOL after excitation at 400 nm. This rise can be well reproduced by an exponential function with a time constant of 1.58 ± 0.08 ps, a value that is identical, within the limit of error, to the S₂ lifetime.

In ACN, the rise time of the S₁ fluorescence is longer and amounts to 2.37 ± 0.08 ps, in agreement with the S₂ lifetime in this solvent (see Figure 4B).

Addition of large amounts of quencher results in a substantial acceleration of the S₂ dynamics as shown in Figure 3A in a 1:1 ACP/TOL mixture ([ACP] = 4.3 M). Moreover, the initial fluorescence intensity is smaller in the presence of quencher,

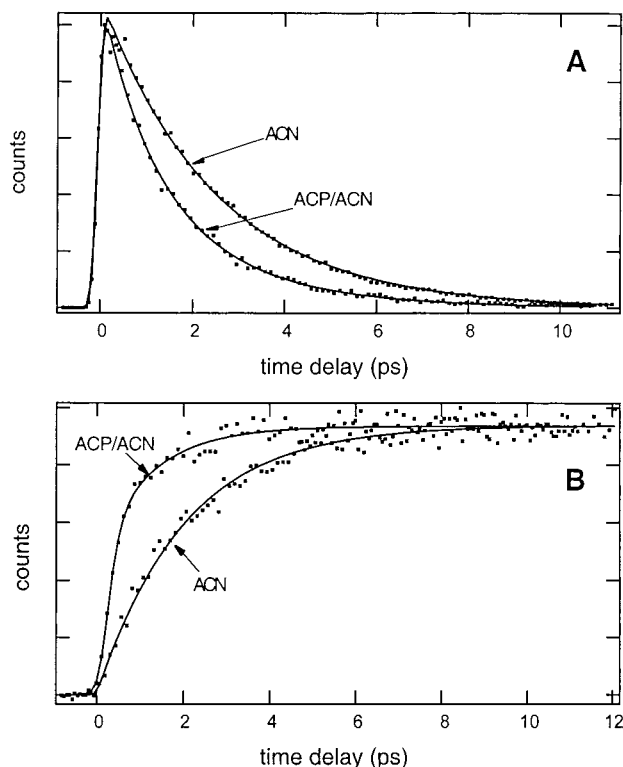


Figure 4. Intensity-normalized time profiles of the fluorescence intensity measured with ZnTPP at 430 nm (A) and 605 nm (B) in ACN and in a 1:1 mixture of ACP/ACN.

TABLE 1: Kinetic Parameters Obtained from the Biexponential Analysis of the S_2 and S_1 Dynamics in 1:1 (v/v) Solvent and Quencher Mixtures^a

quencher/solvent	τ_D^F (fs)	A_D^F (%)	τ_D^S (ps)	τ_R^F (fs)	A_R^F (%)
ACP/ACN	810	60	2.35	430	80
TMB/ACN	390	42	1.40	400	74
ACP/TOL	350	65	1.40	350	85
TMB/TOL	370	60	1.50	460	82

^a τ_D^F and τ_D^S are the lifetimes of the fast- and slow-decaying components of S_2 , and A_D^F and A_D^S are their corresponding amplitudes ($A_D^S = 100 - A_D^F$). τ_R^F is the time constant of the fast-rising component of S_1 with amplitude A_D^F . For the analysis of the S_1 dynamics, the time constant of the slow component was kept equal to τ_D^S ($A_R^S = 100 - A_R^F$) (error on $\tau \approx \pm 5\%$).

although the number of absorbed photons remains constant. The fluorescence dynamics is also more complex and a biexponential function is required to reproduce it. For example, in a 1:1 ACP/ACN mixture, the faster component, which is also the dominant one with 60% of the total amplitude, has a lifetime, τ_D^F , of 810 fs, while the slower component has a lifetime, τ_D^S , of 2.35 ps, close to that measured in pure ACN (see Figure 4). The use of a fixed lifetime of 2.41 ps results in a very good fit to the experimental data as well. The decay times, τ_D^F and τ_D^S , obtained from the analysis of the S_2 fluorescence in 1:1 quencher/solvent mixtures are listed in Table 1. This table shows that τ_D^S is very close to the decay time measured in pure solvents, with the exception of TMB/ACN.

Figure 3B illustrates the effect of ACP on the early dynamics of S_1 fluorescence in TOL. The presence of ACP considerably speeds up the formation of S_1 . However, the maximum intensity of the S_1 fluorescence is independent of the presence of quencher. Contrary to the pure solvent case, a biexponential function has to be used to reproduce this time profile. As the amplitude of the slowest component represents less than 30%

TABLE 2: Free Energies for Charge Separation from ZnTPP*(S_1) and from ZnTPP*(S_2)^a and for Charge Recombination via Paths A and B, and Solvent Reorganization Energies

	ACP/ACN	TMB/ACN	ACP/TOL	TMB/TOL
$\Delta G_{CS}^{S_1}$ (eV)	0.57	0.36	0.70	0.80
$\Delta G_{CS}^{S_2}$ (eV)	-0.28	-0.49	-0.15	-0.05
ΔG_{CR}^A (eV)	-2.62	-2.41	-2.75	-2.85
ΔG_{CR}^B (eV)	-0.57	-0.36	-0.70	-0.80
λ_s (eV)	0.90	0.82	0.68	0.26

^a Calculated from eq 2. $E^*(S_1) = 2.05$ eV, $E^*(S_2) = 2.9$ eV, $E_{ox}(ZnTPP) = 0.80$ V vs SCE,²⁸ $E_{red}(ZnTPP) = -1.30$ V vs SCE,²⁹ $E_{ox}(TMB) = 1.12$ V vs SCE,³⁰ and $E_{red}(ACP) = -1.85$ V vs SCE.³¹

of the total amplitude, the uncertainty on its time constant, τ_R^S , is large. The S_1 rises were first fitted by allowing the amplitude and the time constant of both components to vary. As the resulting values of τ_R^S were quite similar to the longer decay time, τ_D^S , measured at 430 nm, the fits were repeated with τ_R^S kept equal to τ_D^S . The rise times obtained from this analysis are listed in Table 1. The dynamics of S_1 fluorescence at longer time is not influenced by the presence of ACP. Indeed, the ultrafast rise is followed by a single-exponential decay with a time constant of 1.8 ns, in agreement with the literature.^{25,26}

Qualitatively similar behavior is observed in 1:1 ACP/ACN (see Figure 4B), TMB/ACN, and TMB/TOL mixtures. The time constants obtained from the biexponential fit are listed in Table 1.

Discussion

The above results can be explained with a scheme where ET quenching of ZnTPP*(S_2) by Q results to the formation of a high-lying GIP, which itself decays by CR to ZnTPP*(S_1) + Q via path B (see Figure 1). If CR were occurring along path A, the quenching of S_2 fluorescence would also be accompanied by a quenching of S_1 fluorescence, contrary to the observation (see Figure 2).

Energetics. The free energy of formation of the GIP in solvent mixtures, ΔG_{GIP} , can be estimated from²⁷

$$\Delta G_{GIP} = E_{ox}(D) - E_{red}(A) - \frac{e^2}{4\pi\epsilon_0 75} \left(\frac{1}{r_+} + \frac{1}{r_-} \right) + \frac{e^2}{8\pi\epsilon_0 \epsilon_s} \left(\frac{1}{r_+} + \frac{1}{r_-} - \frac{2}{d} \right) \quad (1)$$

where $E_{ox}(D)$ and $E_{red}(A)$ are the oxidation and reduction potentials of the donor and the acceptor in ACN, respectively; r_+ and r_- are the ionic radii; d is the interionic distance; and ϵ_s is the dielectric constant of the medium. In this equation, the solvation free energy of the ions in ACN ($\epsilon_s = 37.5$), which is implicitly contained in the redox potentials, is removed and replaced by the free energy of solvation in the solvent mixture. The last term on the right-hand side of eq 1 also contains the electrostatic interaction between the ions at a distance d .

The free energy for the CS process (ET quenching) is then given by

$$\Delta G_{CS} = \Delta G_{GIP} - E^* \quad (2)$$

where E^* is the energy of the excited state.

On the other hand, the free energy for CR to the neutral ground state via path A is simply $\Delta G_{CR}^A = -\Delta G_{GIP}$.

Table 2 shows the ΔG_{CS} values calculated for the quenching of ZnTPP*(S_1) and ZnTPP*(S_2) by ACP and TMB in ACN and TOL (1:1 mixtures). For these calculations, ϵ_s was taken as the average dielectric constant of the solvent and of the quencher,³²

and contact distance was assumed. The radii were calculated by assuming spherical ions. Their volumes were determined by using the van der Waals increment method.³³

In the quenching by ACP, ZnTPP*(S₂) acts as an electron donor, while in the ET with TMB, ZnTPP*(S₂) is the electron acceptor. The numbers listed in Table 2 indicate that CS is only energetically favorable if ZnTPP is in the S₂ state, the quenching of ZnTPP*(S₁) being clearly endergonic. These values should only be considered as a rough indication of the feasibility of ET quenching. Indeed, a precise calculation of ΔG_{GIP} would require us to take into account the actual shape of the reactants and to know the exact solvent composition around ZnTPP. Nevertheless, the results presented here confirm that the GIP states are located between the ZnTPP*(S₂) + Q and ZnTPP*(S₁) + Q states.

Charge Separation. To ensure efficient ET quenching during the very short lifetime of ZnTPP*(S₂), high concentrations of quenchers have to be used. Indeed, the S₂ lifetime is so short that translational and even rotational diffusion are essentially frozen. Consequently, the multiexponential decay of the S₂ fluorescence reflects the distribution of different donor/acceptor distances and mutual orientations. For example, the component with a lifetime equal to that measured without quencher (see Table 1) can be ascribed to the ZnTPP*(S₂) population without a quencher molecule at a proper distance and orientation for ET within the S₂ lifetime. With TMB/ACN, the time constant of the slow S₂ decay component is smaller than the S₂ lifetime in pure ACN, indicating that ET quenching with less favorable donor–acceptor geometry is probably also operative but less efficient. The fact that this slower ET quenching component is not observed with the other systems might be due to the smaller driving force for CS in these mixtures (see Table 2). Similar multiexponential decays have been reported for ET quenching in electron-donating solvents.^{34,35}

As mentioned above, the initial intensity of the S₂ fluorescence decreases substantially with increasing quencher concentration. Moreover, the strong decrease of the S₂ fluorescence quantum yield observed in the steady-state spectrum can be only *partially* accounted for by the shortening of S₂ lifetime measured by upconversion. These two observations indicate that there must be an additional decay component of S₂, which is too fast to be measured with the time resolution of our setup. According to numerical simulations, decay components with a lifetime smaller than about 100 fs could account for this difference. Inter-molecular CS processes with time constants smaller than 100 fs have already been observed, for example, in electron-donating solvents^{36,37} or in polymers,³⁸ and therefore such an ultrafast ET is not unrealistic.

Charge Recombination. The absence of any effect of the quenchers on the S₁ fluorescence intensity is a clear proof that CR occurs via path B (see Figure 1), i.e., leads to the formation of ZnTPP*(S₁). If this were not the case, the S₁ fluorescence would also be quenched, contrary to our observation. Consequently, information on the dynamics of this CR process can be obtained from the early dynamics of S₁ fluorescence.

As the formation kinetics of S₁ depends on two consecutive processes, i.e., CS followed by CR, two limiting cases should be considered:

(1) If CR is much slower than CS, the rise of S₁ should be much slower than the S₂ decay and directly reflect the CR dynamics.

(2) If CR is much faster than CS, the rise time of S₁ should be almost equal to the S₂ lifetime and no quantitative information on the CR dynamics can be extracted.

Table 1 shows that, apart from ACP/ACN, the rise time of the S₁ fluorescence, $\tau_{\text{R}}^{\text{F}}$, is very similar to the time constant of the fast S₂ decay component, $\tau_{\text{D}}^{\text{F}}$. For these systems, the limiting case 2 seems to apply.

For ACP/ACN, however, most of the rise of the S₁ fluorescence is substantially faster than the decay of S₂. This apparently contradictory observation is actually further evidence for the existence of an ultrafast (<100 fs) decay component of S₂, as discussed above. If a substantial fraction of the S₂ population is quenched in less than 100 fs, the measured 430 fs S₁ rise time could reflect the CR of the resulting GIPs (case 1). This ultrafast CS process is apparently also operative in the other mixtures. Consequently, the S₁ rise time measured with these systems might as well correspond to CR of this GIP population. In this case, the similarity between $\tau_{\text{D}}^{\text{F}}$ and $\tau_{\text{R}}^{\text{F}}$ would be coincidental. At present, we do not have enough information to decide between these two possibilities.

In any case, the time scale of CR is much faster than that of diffusion and therefore the mutual orientation of the ions in the pair must be very similar to that of the reactants during the CS. Consequently, multiexponential CR dynamics can be expected and the values listed in Table 1 must only be considered as average time constants. The slower-rising component of S₁ can be due either to the fraction of ZnTPP*(S₂) that has not been quenched or to the CR of GIPs with a less favorable geometry. However, it is quite clear that most of the CR to ZnTPP*(S₁) + Q is ultrafast and occurs in less than 500 fs, independently on the quencher and on the solvent.

According to Marcus theory,¹ such ultrafast ET processes are predicted to occur in the barrierless regime, i.e., in the region where the sum of free energy and of the total reorganization energy, λ , vanishes. The reorganization energy contains a contribution of the high-frequency intramolecular modes, λ_{v} , and of the low-frequency modes, due mainly to the solvent, λ_{s} . For CR of aromatic radical ions, λ_{v} is typically of the order of 0.2–0.4 eV.^{39,40,13} According to the dielectric continuum theory, λ_{s} depends on the ionic radii, on the interionic center-to-center distance, and on the solvent polarity.¹ The λ_{s} values calculated from the average dielectric constants of the quencher and of the solvent and assuming spherical ions and contact distance are listed in Table 2. The total reorganization energy in the first three mixtures, the polar mixtures, can be expected to be larger than 1 eV. According to these values, the CR in these mixtures should occur in the normal regime but not very far from the barrierless region. Considering that the time scale of CR is similar to those of vibrational relaxation and solvation, the actual energy gap for CR and the effective reorganization energies might be different from those calculated above, assuming reactant and product states in thermal equilibrium. Indeed, we have recently shown that CR of GIPs formed upon highly exergonic ET quenching can occur during vibrational relaxation.³⁹

Despite this, it is quite clear that the free energy for CR to the neutral ground state, i.e., via path A, is very high and much larger than the total reorganization energy. In this case, CR should occur in the inverted region and therefore should be considerably slower than those measured here. For example, CR of GIPs with similar energies have been reported to take place with time constants of the order of 100 ps to 1 ns.³⁹ With the systems studied here, this slow CR pathway can clearly not compete with that leading to the excited product.

Concluding Remarks

The above results clearly prove that a highly exergonic ET reaction can result in the formation of an electronically excited

product. The Marcus inverted region has been predominantly observed with CR processes.^{11–13} In those cases, there is no accessible state between the GIP and the neutral ground state. The present investigation shows unambiguously that the presence of an excited state, accessible via a spin-allowed process and located between the GIP and the neutral ground state, suppresses the occurrence of the Marcus inverted region. The effect of a low-lying excited state of the product is to shift the process from the inverted toward the barrierless regime. There is no evident reason why this phenomenon, observed here in a charge recombination process, would not occur as well in a charge separation reaction, if an electronic excited state of the product is located below the initial state, $M^* + Q$. The radical ions of the aromatic compounds used in ET quenching experiments have electronic excited states below 1.6 eV. Consequently, these excited states could be efficiently populated when $\Delta G_{ET} < -2$ eV. However, for the reasons described in the Introduction, their direct observation in a ET process remains a challenging task, which certainly requires first a better knowledge and understanding of their dynamics.

Finally, such GIPs located above an electronic state of the product allow the investigation of the dynamics of weakly and moderately exergonic CR processes. They are also good systems to study the interplay between ET and vibrational relaxation.

Acknowledgment. This work was supported by the Fonds National Suisse de la recherche Scientifique through Project 2000-0632528.00.

References and Notes

- Marcus, R. A.; Sutin, N. *Biochim. Biophys. Acta* **1985**, *811*, 265.
- Rehm, D.; Weller, A. *Isr. J. Chem.* **1970**, *8*, 259.
- Closs, G. L.; Miller, J. R. *Science* **1988**, *240*, 440.
- Tachiya, M.; Murata, S. *J. Phys. Chem.* **1992**, *96*, 8441.
- Mataga, N.; Kanda, Y.; Asahi, T.; Miyasaka, H.; Okada, T.; Kakitani, T. *Chem. Phys.* **1988**, *127*, 239.
- Hug, G. L.; Marciniak, B. *J. Phys. Chem.* **1995**, *99*, 1478.
- Breslin, D. T.; Fox, M. A. *J. Phys. Chem.* **1994**, *98*, 408.
- Gumy, J.-C.; Vauthey, E. *J. Phys. Chem. A* **1997**, *101*, 8575.
- Brodard, P.; Sarbach, A.; Gumy, J.-C.; Bally, T.; Vauthey, E. *J. Phys. Chem. A* **2001**, *105*, 6594.
- Shida, T. *Electronic Absorption Spectra of Radical Ions*; Physical Sciences Data, Vol. 34; Elsevier: Amsterdam, 1988.
- Mataga, N.; Asahi, T.; Kanda, Y.; Okada, T.; Kakitani, T. *Chem. Phys.* **1988**, *127*, 249.
- Vauthey, E.; Högemann, C.; Allonas, X. *J. Phys. Chem. A* **1998**, *102*, 7362.
- Gould, I. R.; Moody, R.; Farid, S. *J. Am. Chem. Soc.* **1988**, *110*, 7242.
- Haselbach, E.; Vauthey, E.; Suppan, P. *Tetrahedron* **1988**, *44*, 7335.
- Gschwind, R.; Haselbach, E. *Helv. Chem. Acta* **1979**, *62*, 941.
- Hubig, S. M.; Bockman, T. M.; Kochi, J. K. *J. Am. Chem. Soc.* **1997**, *119*, 2926.
- Högemann, C.; Vauthey, E. *J. Phys. Chem. A* **1998**, *102*, 10051.
- Levin, P. P.; Pluzhnikov, P. F.; Kuzmin, V. A. *Chem. Phys. Lett.* **1988**, *147*, 283.
- Vauthey, E.; Henseler, A. *J. Phys. Chem.* **1995**, *99*, 8652.
- Weller, A.; Zacchariasse, K. In *Chemiluminescence and bioluminescence*; Cornier, M., Hercules, D. M., Lee, J., Eds.; Plenum Press: New York, 1973; p 169.
- Muller, P.-A.; Vauthey, E. *J. Phys. Chem. A* **2001**, *105*, 5994.
- Kalyanasundaram, K. *Photochemistry of polypyridine and porphyrin complexes*; Academic Press: San Diego, CA, 1992.
- Kobayashi, H.; Kaizu, Y. In *Porphyrins: Excited States and Dynamics*; Gouterman, M., Rentzepis, P., Straub, K. D., Eds.; American Chemical Society: Washington, DC, 1986; Vol. 321, p 105.
- Gruszadyan, G. G.; Tran-Thi, T.-H.; Gustavsson, T. *Proc. SPIE* **2000**, *4060*, 96.
- Brodard, P.; Matzinger, S.; Vauthey, E.; Mongin, O.; Papamicaël, C.; Gossauer, A. *J. Phys. Chem. A* **1999**, *103*, 5858.
- Hsiao, J. S.; Krueger, B. P.; Wagner, R. W.; Johnson, T. E.; Delaney, J. K.; Mauzerall, D. C.; Fleming, G. R.; Lindsey, J. S.; Bocian, D. F.; Donohoe, R. J. *J. Am. Chem. Soc.* **1996**, *118*, 11181.
- Weller, A. *Z. Phys. Chem. N.F.* **1982**, *133*, 93.
- Wolberg, A.; Manassen, J. *J. Am. Chem. Soc.* **1970**, *92*, 2982.
- Seely, G. R.; Gust, D.; Moore, T. A.; Moore, A. L. *J. Phys. Chem.* **1994**, *98*, 10659.
- Siegerman, H. In *Techniques of Chemistry*; Weinberg, N. L., Ed.; Wiley: New York, 1975; Vol. V, p 667.
- Julliard, M.; Chanon, M. A. *Chem. Rev.* **1983**, *83*, 425.
- Riddick, J. A.; Bunger, W. B. *Organic Solvents*; Wiley: New York, 1970.
- Edward, J. T. *J. Chem. Educ.* **1970**, *4*, 261.
- Nagasawa, Y.; Yartsev, A. P.; Tominaga, K.; Johnson, A. E.; Yoshihara, K. *J. Chem. Phys.* **1994**, *101*, 5717.
- Castner, E. W., Jr.; Kennedy, D.; Cave, R. J. *J. Phys. Chem. A* **2000**, *104*, 2869.
- Xu, Q.-H.; Scholes, G. D.; Yang, M.; Fleming, G. R. *J. Phys. Chem. A* **1999**, *103*, 10348.
- Seel, M.; Engleitner, S.; Zinth, W. *Chem. Phys. Lett.* **1997**, *275*, 363.
- Brabec, C. J.; Zerza, G.; Cerullo, G.; De Silvestri, S.; Luzzati, S.; Hummelen, J. C.; Sariciftci, S. *Chem. Phys. Lett.* **2001**, *340*, 232.
- Vauthey, E. *J. Phys. Chem. A* **2001**, *105*, 340.
- Kikuchi, K.; Takahashi, Y.; Hoshi, M.; Niwa, T.; Katagiri, T.; Miyashi, T. *J. Phys. Chem.* **1991**, *95*, 2378.